Active control of oscillatory thermocapillary convection

Junichiro Shiomi, Gustav Amberg, and Henrik Alfredsson
Department of Mechanics, Royal Institute of Technology (KTH), S-100 44 Stockholm, Sweden
(Received 4 November 2000; published 30 August 2001)

Active control of oscillatory thermocapillary flow was applied in an open cylindrical container filled with silicone oil. Thermocapillary convection was driven by imposing a radial temperature gradient on a flat free surface. The control was realized by locally heating the surface at a single position using the local temperature signal at a different position fed back through a simple algorithm. Significant attenuation of the oscillation was achieved in a wide range of supercritical Marangoni numbers, with the best performance in the weakly non-linear regime. Simultaneously measuring the temperature oscillation at two positions gives us a good insight in how the control influences the whole temperature field on the free surface. Quantitative analysis was done to characterize the optimal feedback amplification and the required power.

DOI: 10.1103/PhysRevE.64.031205 PACS number(s): 47.20.Dr, 47.62.+q, 47.20.Ky, 81.10.−h

I. INTRODUCTION

In the production of single crystals, the containerless processing has advantages in order to increase the purity of the crystal. In the float-zone method, where a raw material rod is slowly pulled through a ring heater, the small zone near the heater is molten and resolidified as a single crystal. This system has been proposed for space processing, since the flow in the melt is influenced by gravitational convection. Experiments in microgravity conditions revealed that even with the absence of buoyancy, thermocapillary convection could be significant. Furthermore, the time-dependent oscillatory state of the thermocapillary convection was found to cause detrimental striations in the chemical composition of the finished crystal.

Thermocapillary convection is a fluid motion driven by the variation of surface tension with temperature. The basic mechanism can be understood by considering a horizontal force balance over a small piece of the interface. The difference in surface tension can be balanced only by the viscous shear stress, which implies that the fluid is set into motion. The strength of the driving force of the convection is commonly characterized by Marangoni number (Ma), the ratio between convection and thermal diffusion. It is well known that the flow experiences a transition from two-dimensional steady flow to three-dimensional time-dependent flow at a well defined critical Marangoni number.

Industrial need has motivated a number of studies to clarify the onset mechanism of the instability. A convective instability, named hydrothermal-wave instability, was theoretically identified on shallow plane fluid layers by Smith and Davis [1]. A temperature disturbance wave was found to propagate in a direction that is dependent on the Prandtl number of the liquid. Later, for a high Prandtl number (Pr) fluid, this was experimentally demonstrated by Riley and Neitzel [2].

Many experimental studies have been done on the half-zone model, where a liquid drop is held between two coaxial rods that are maintained at different temperatures to impose axial temperature gradients on the free surface [4,5]. The oscillatory thermocapillary flow was detected first by Schwabe and Scharmann [3] and Chun and Wuest [6]. Later, Preisser *et al.* [7] showed that the azimuthal wave number and frequency are determined by the aspect ratio of the liquid zone.

Kamotani *et al.* [8] first demonstrated the thermocapillary oscillation in a cylindrical container of the annular type for high Pr. A three-dimensional (3d) oscillatory flow with a periodic surface temperature pattern was obtained. Comparing the data in normal gravity with data obtained in microgravity where the container size was varied, the upper limit of the container size below which Marangoni convection dominates over buoyancy convection was identified [9,10].

The onset of oscillatory thermocapillary flow was studied numerically by a linear stability theory by Neitzel *et al.* [11] and Kuhlmann and Rath [12]. Kazarinoff and Wilkowski [13,14] made numerical simulations of 2D axially symmetric full float zone. Rupp *et al.* [15] presented a three-dimensional simulation of a half zone with an aspect ratio of 0.6 and found $m=2$ to be the most dangerous mode. The mechanism for the onset of oscillatory flow in a half zone for a low Prandtl number liquid was identified by Levenstam and Amberg [16] as a purely hydrodynamic instability, very similar to the instability of a ring. Wanschura *et al.* [17] made similar interpretations of the linear stability for a high Prandtl number liquid.

Based on these fundamental studies, the present work focuses on active control of the oscillatory thermocapillary convection. There are only a few reported works of active control of thermocapillary convection. An attempt to stabilize the thermocapillary wave instability in an experiment on a plane fluid layer has been made by Benz *et al.* [18]. The temperature signal sensed by a thermocouple near the cold end of the layer was fed forward to control a laser that heated the fluid surface along a line.

For an axisymmetric base state, Petrov *et al.* [19] attempted to stabilize oscillations in a half zone, by applying a nonlinear control algorithm using local temperature measurement close to the free surface and heating a thermoelectric element placed at a location diametrically opposite the measurement. A successful control was reported for Ma $=17\,750$, but the control scheme failed for Ma$\geqslant 19\,000$ because of the strong nonlinearity of the dynamics. The oscillations could be suppressed at the sensor, however infrared

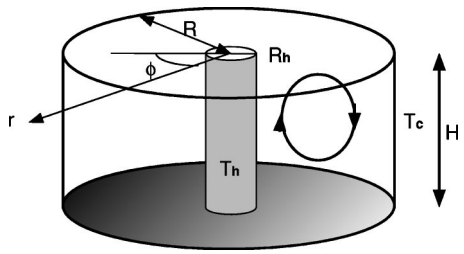

FIG. 1. Geometry.

visualization revealed the presence of standing waves with antinodes of the feedback element and the sensor.

The aim of this work is to control the oscillatory thermocapillary flow by using a temperature sensor and a wire heater in the related cylindrical geometry. The control was realized by locally heating the surface at a single position using the local temperature signal at different position fed back through a simple algorithm.

II. EXPERIMENT

A generic flow of a character similar to that found for instance in the float-zone method is studied [8]. As shown in Fig. 1, the system is an open cylindrical container filled with liquid to have a flat-free upper surface. A heated pipe with a prescribed temperature is located on the axis of the container. The outer cylindrical wall is maintained at a lower temperature. Thermocapillary convection is thus driven by imposing a radial temperature gradient on the flat-free surface. The bottom temperature condition is adiabatic. The major advantage of this geometry is that having the free surface perpendicular to gravity, it can be kept flat, thus better quantitative analysis can be achieved. This system is also an attractive object for control since its closed geometry makes feedback control possible.

The Marangoni number is defined as

$$\mathrm{Ma}=\frac{\gamma \Delta T R}{\mu \alpha}, \tag{1}$$

$$\Delta T=T_h-T_c, \tag{2}$$

where γ, α, and μ are the surface tension coefficient, thermal diffusivity, and dynamic viscosity, respectively. T_h and T_c are the temperatures of the hot and cold walls. The temperature is nondimensionalized as

$$\theta=\frac{T-T_c}{\Delta T} \tag{3}$$

throughout the analysis.

The experimental apparatus is shown in Fig. 2. The test cell consists of a copper cylinder with an inner radius $R=3$ mm, a thin coaxial pipe heater, and an insulated bottom made of Teflon. The cell diameter is small enough to have the thermocapillary force dominate the buoyancy force [10]. The cell is filled with 1cS silicone oil with a Prandtl number around 14. In order to obtain a flat-free surface, the heater pipe was machined to have a smaller diameter above the surface. Then the parts of the pipe heater and the copper

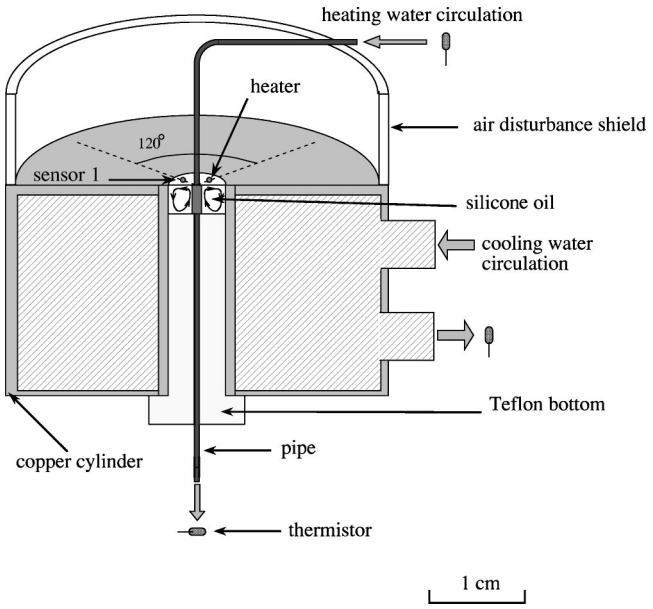

FIG. 2. Experimental setup.

cylinder above the surface were coated with Fluorad (3M Scotchguard). This inhibits the liquid from wetting the lips, thus the contact lines can be pinned. A temperature gradient is imposed along the free surface by circulating warm water through the pipe heater and cold water through the copper cylinder. The aspect ratio of the test section $\mathcal{R}_A$, defined as the ratio between the height of fluid H and the radius of the cell R, is kept at 1 throughout the experiments. The ratio of diameter of the heated pipe R_h to R is $\mathcal{R}_H=0.21$. To keep the volume and the free surface shape constant, the evaporation of the liquid is compensated by connecting a relatively large container filled with the same liquid to the bottom of the cell through a very thin hole.

Many reported experimental works to determine the onset of the instability have encountered difficulties in the quantitative accuracy of measuring the amplitude of the oscillations. The temperature oscillation is commonly measured by contact-less techniques such as thermographs or placing thermocouples close to the free surface of the liquid. An alternative way is to dip the thermocouples into the liquid, which may contaminate the flow field because thermocouples are rather large especially for the ground-based experiments where the system is made very small to let the thermocapillary force dominate over buoyancy force. Either way, the quantitative temperature measurement is difficult, especially for the small temperature fluctuations close to criticality that is essential to determine the critical Marangoni number.

In the present work, the local temperatures at two positions are simultaneously measured by installing two calibrated cold-wire sensors with diameter $d=2.5$ μm and length $l=0.3$ mm through the free surface. The sensor has a shape of U, where the curved bottom is made of a platinum wire. When the sensor is installed through the surface, the tip of the sensor reaches as far as 100 μm from the surface. The principle is to have a constant current pass through the platinum wire and detect the resistance that is proportional to the temperature. The amount of imposed current is limited so

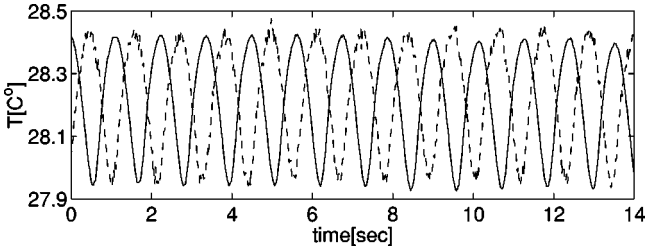

FIG. 3. Temperature signals from two sensors placed with 60° difference in the azimuthal direction. Solid line, sensor 1; dashed line, sensor 2.

that the heating power of the sensor does not exceed 1 μW. Since the wire is very thin, it can be installed through the free surface without causing any appreciable deformation.

The control heater is made in the same manner as for the sensor except for a few differences. In order to achieve the necessary power output, the heater is made slightly longer ($l=0.5$ mm, $d=2.5$ μm) with 10% rhodium-platinum wire that has more resistance per unit area than pure platinum. Then the heater is placed above the surface within a distance less than 100 μm. The power output from the heater is obtained by measuring current and voltage over the heater.

Sensor 1 and sensor 2 were positioned at $\phi=0°$ and $\phi=-60°$, respectively. The radial position was $r=R_h+(R-R_h)/2$ for both sensors. In the annular configuration, $\mathcal{R}_H$ and $\mathcal{R}_A$ determine the azimuthal wave number of the thermocapillary oscillation. For this particular geometry ($\mathcal{R}_A=1$, $\mathcal{R}_H=0.21$), examining the phase shift between the temperature signals from the sensors 60° apart in azimuthal direction to be out of phase, the oscillation has been found to have the azimuthal wave number of 3 (Fig. 3). This has been confirmed by the flow visualization (Fig. 4). The flow was seeded with flakes (Irodin 120 Pearl Lustre) and illuminated from above. The white part is where the seeded flakes, lying parallel to the surface, reflected the illumination the most. The deformation of the vortex ring was observed to have a triangular shape, which confirms that the azimuthal wave number was 3. Hence, placing the heater 120° away in the azimuthal direction from sensor 1, $(r,\phi)=[R_h+(R-R_h)/2,120°]$, temperature oscillations at the positions would be in phase. A simple cancellation scheme is then realized by applying a voltage proportional to the inverted temperature fluctuation at sensor 1 to the heater. Thus the heater delivers heat locally when the oscillation has a cold spot at the heater location. The minimum heater output power is set to 0 to avoid affecting the base flow by raising the mean temperature. It was made sure that when the control is turned off, the temperature oscillation goes back to the original uncontrolled state. Also the mean temperature has the original value after control is turned off, indicating that the heat delivered to the fluid during control is sufficiently small not to alter the base state appreciably. The ratio of imposed heater voltage to voltage output from sensor 1, the feedback amplification, is set manually. For each Ma, the feedback amplification is varied to find its optimal value, where the most successful control is achieved. The performance of the control scheme is characterized by means of the ratio of the amplitude of oscillation with control to the one without. The amplitudes of the oscillations are obtained as

$$\hat{\theta}=2\sqrt{2}\,\theta_{rms}, \tag{4}$$

where θ_{rms} is the root mean square value of θ. θ_{rms} is computed by taking the square root of the integration of the power spectrum density for more than 20 periods of the oscillation.

For the presented parameter range, we observed traveling waves as shown in Fig. 4, even though there remains an uncertainty of judgment specially close to the criticality. In the case of a traveling wave, the signal measured at a fixed r,ϕ will have a well defined amplitude, independent of ϕ. As for the r dependency of the oscillation amplitude, Lavalley *et al.* [21,22] performed a 3D numerical simulation in the same system as the present experiment and showed surface isotherms indicating that the amplitude of the oscillation has a broad maximum around the center between the hot pipe and the cold wall. Then, in this regime, the precise radial positions of the sensors and the heater are not crucial for the control scheme to function. Hence, the radial locations of the sensors and the heater were decided to be in the center of the gap also for the sake of experimental convenience.

Sensor 2 is kept at $(r,\phi)=[R_h+(R-R_h)/2,120°]$ during the control to observe the azimuthal wave number. This also gives a good insight into how the control influences the whole temperature field.

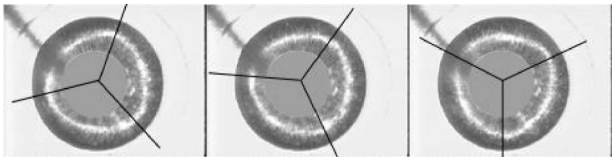

FIG. 4. Flow visualization of the horizontal section $(\epsilon,\mathrm{Ma},\mathrm{Ma}_{cr})=(0.6,5040,3150)$ [21,22].

III. RESULTS

The control scheme is applied to flows for various $\epsilon=(\mathrm{Ma}-\mathrm{Ma}_{cr})/\mathrm{Ma}_{cr}$, where Ma_{cr} is the critical Marangoni number. Determination of the critical Marangoni number is based on bifurcation analysis, which suggests that the nondimensionalized amplitude of the oscillation should be proportional to the square root of ϵ for a supercritical Hopf bifurcation [20]. A square root curve is fit to the experimental data, giving the points close to the bifurcation a large weight. The curve is extrapolated down to $\epsilon=0$ to find Ma_{cr} as 3201. In Fig. 5, $\hat{\theta}_0$ which is the amplitude $\hat{\theta}$ of the uncontrolled oscillation is plotted for a range of ϵ with the bifurcation curve. The bifurcation curve fits the experimental points well in the weakly nonlinear regime ($\epsilon\ll 1$), which assures the reliability of the performed temperature measuring technique. The points fall below the curve as the nonlinearity becomes stronger [$\epsilon\sim O(1)$].

In Fig. 6, the time history of the temperature signal at sensor 1 position and the corresponding heater output power is shown for $\epsilon=0.11$. When the control is turned on, the

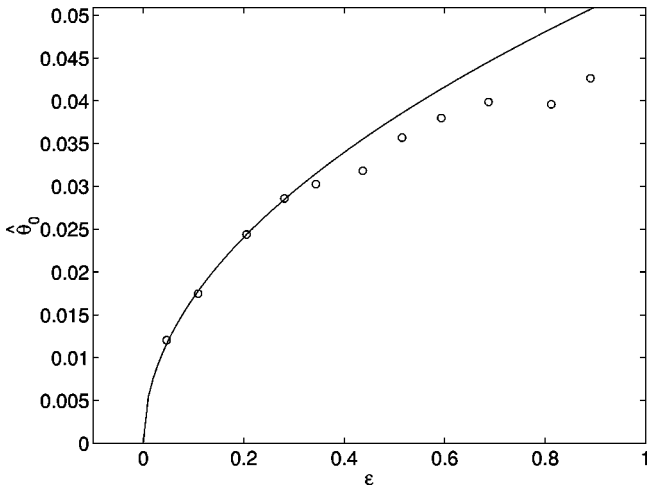

FIG. 5. Bifurcation analysis of the uncontrolled signal at sensor 1. $(r,\phi)=[R_h+(R-R_h)/2,0°]$. $\hat{\theta}_0$: The amplitude $\hat{\theta}$ of the oscillation without control, $\epsilon=(\mathrm{Ma}-\mathrm{Ma}_{cr})/\mathrm{Ma}_{cr}$.

amplitude of the temperature oscillation is quickly suppressed to 10–20 %. The initial transient has a duration of a few seconds. Once the periodic signal is stabilized, the heater power drops down to less than 10% of its initial value. Removing the control, the system goes back to the uncontrolled state over a period of about 30 s. This control can be maintained for infinite time, and is quantitatively repeatable.

Figure 7 is plotted in the same manner as Fig. 6 for $\epsilon=0.69$, a parameter in the strongly nonlinear regime. Applying the control, the amplitude of the oscillation is reduced significantly in a few seconds. However, the reduction of the amplitude is much less than for the weakly nonlinear case, $\epsilon=0.11$. The controlled signal has an envelope, a low frequency ($\sim$0.05 Hz) modulation of the oscillation amplitude. A corresponding periodic increase is observed in the

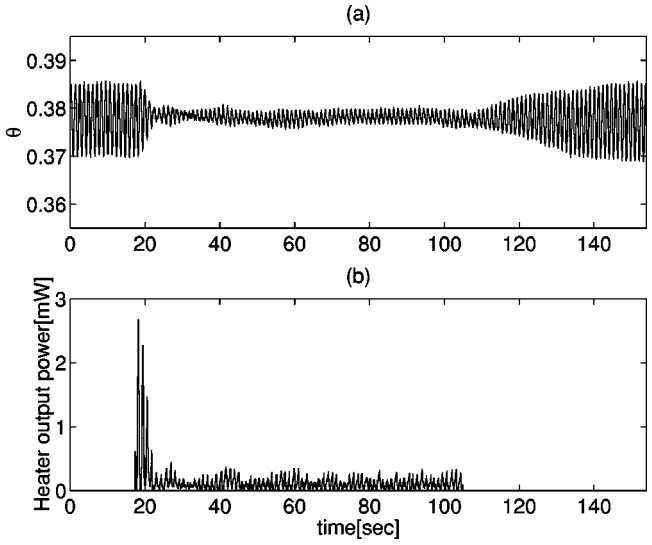

FIG. 6. (a) Time history of the temperature signal obtained from sensor 1. $\theta=(T-T_c)/\Delta T$, where T, local temperature; T_c, cold wall temperature; ΔT, imposed temperature difference. (b) Simultaneously measured heater output power, $\epsilon=0.11$.

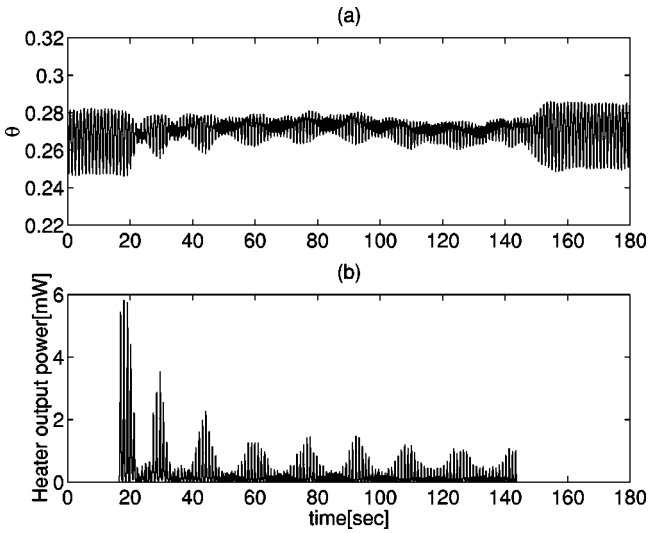

FIG. 7. (a) Time history of the temperature signal obtained from sensor 1. (b) Simultaneously measured heater output power, $\epsilon=0.69$.

heater output power. This implies the existence of two waves with slightly different frequency being superimposed. An attempt to damp the envelope by raising the feedback amplification merely resulted in an amplification of the fluctuation. When the control is removed, the envelope disappears and the amplitude increases to its original value in about 10 s.

The power spectra for the signals in Figs. 6 ($\epsilon=0.11$) and 7 ($\epsilon=0.69$) are shown in Figs. 8 and 9, respectively. The dashed curves show the spectra with control, solid curves show the ones without control. Taking the energy around the peaks into account, the first harmonics are amplified while the others are damped in both figures. Especially when the nonlinearity of the uncontrolled oscillation is strong ($\epsilon=0.69$), the energy around the first harmonic is comparable to the one around the fundamental frequency. The nature of the control scheme suggests that the control should be able to damp any overtones to some extent as long as they originate

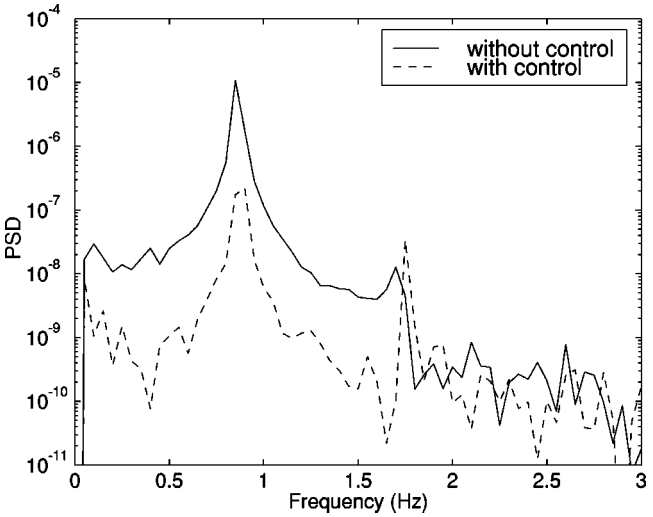

FIG. 8. The power spectrum density for the temperature signal without control (solid line) and with control (dashed line), $\epsilon=0.11$.

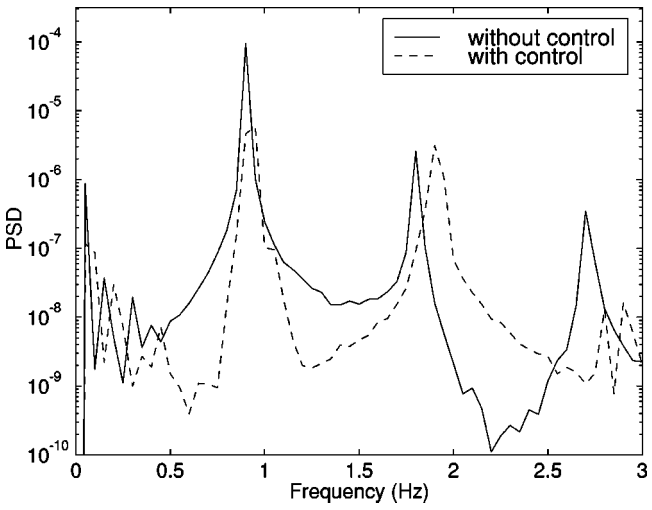

FIG. 9. The power spectrum density for the temperature signal without control (solid line) and with control (dashed line), $\epsilon=0.69$.

from oscillations that are in phase at sensor 1 and the heater. In this regard, the energy around the first harmonic is not purely detected from the mode-3 oscillation. It must originate from the oscillation, which has a spatial structure that is amplified by the control scheme.

A better view is obtained from the wavelet analysis for $\epsilon=0.69$ shown in Fig. 10. For each time step, the amplitude is normalized with its maximum value so that the change of the dominant frequency component over time can be examined. It is shown that the fundamental frequency is dominant at the peaks of the envelope while the first harmonic is dominant at the nodes. This means that the first harmonic remains uncontrolled while the fundamental frequency is successfully reduced.

In both the high and the low ϵ cases, the power spectrum density of the fundamental frequency (~ 1 Hz) is decreased by the control. Furthermore, as it was expected from the

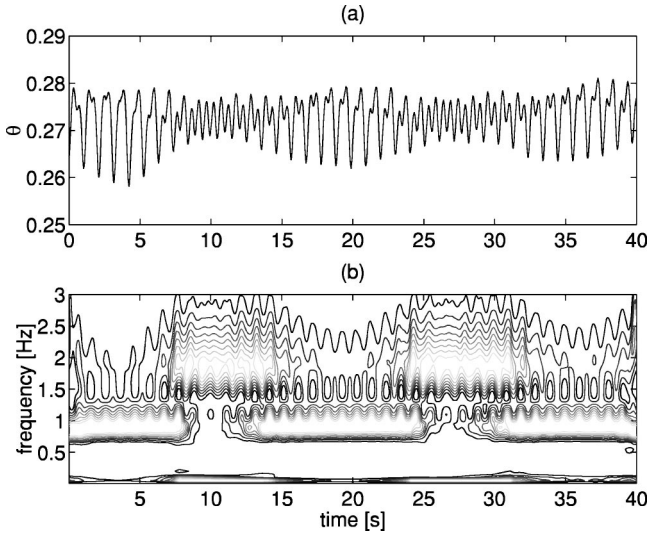

FIG. 10. (a) Focused view of the temperature signal for $\epsilon=0.69$ [Fig. (7a)]. (b) Contour line representation of the wavelet analysis. Data were scaled with their maximum in each time step.

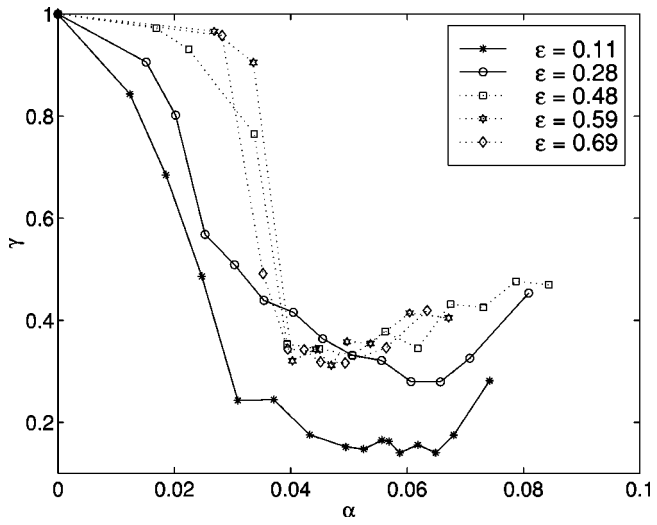

FIG. 11. The analysis of optimal amplification for a range of ϵ.

modulation observed in the controlled signal for $\epsilon=0.69$, there are two frequency components lying close to each other that is forming a flat peak around the base frequency. The difference between the two edges correspond to the frequency (0.05 Hz) of the modulation. The experiments carried out in the same set up by Lavalley *et al.* [21,22] suggests that the origin of the new frequency component be mode 2. They have shown that a slight change in $\mathcal{R}_H$ from 0.21 to 0.16 causes the transition in mode number from 3 to 2. This implies that, for the given geometry ($\mathcal{R}_A=1,\mathcal{R}_H=0.21$), the potential for both modes to dominate the flow is comparable. Therefore when the mode-3 oscillation is suppressed, the next dangerous mode, mode 2, may appear. The frequency of mode 2 was identified by Lavalley *et al.* [21,22] to be around 1 Hz that corresponds to the frequency of the newly emerged mode.

For each ϵ, the optimal feedback amplification is obtained by gradually increasing the gain,

$$G=\frac{U_{heater}}{U_{sensor\ 1}}, \tag{5}$$

where U_{heater} is the imposed heater voltage and $U_{sensor\ 1}$ is the output voltage from sensor 1. Optimal gain ($G_{optimal}$) is defined to give minimum γ, where

$$\gamma=\frac{\hat{\theta}_{controlled}}{\hat{\theta}_0}. \tag{6}$$

$\hat{\theta}_{controlled}$ is $\hat{\theta}$ calculated from the controlled oscillation. The scheme gradually loses the control as G exceeds $G_{optimal}$. A gain factor α is introduced as scaling of G as

$$\alpha=G\hat{\theta}_0. \tag{7}$$

In Fig. 11 γ is plotted against α, where the points in the weakly and strongly nonlinear regimes are described with a solid line and dotted line, respectively.

In the strongly nonlinear regime, the lines collapse onto each other. In this regime, the G necessary for the control to

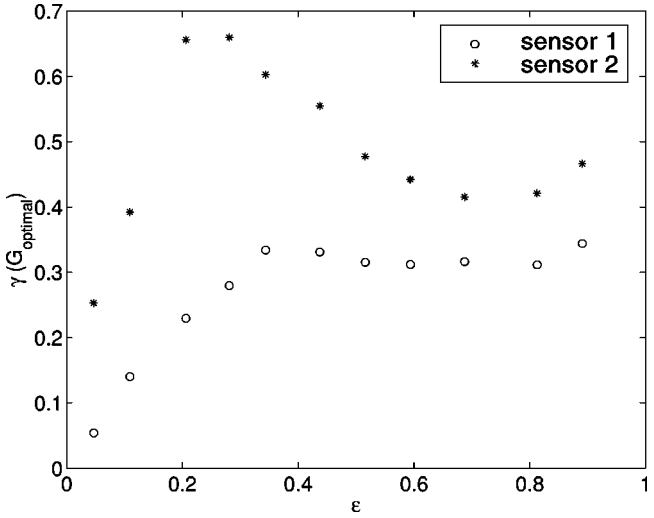

FIG. 12. Performance of the control over a range of ϵ. ϵ, overcritical parameter; $\gamma(G_{optimal})$, ratio of Fourier amplitude with control to amplitude without control when $G=G_{optimal}$. Circles, sensor 1 signal; stars, sensor 2 signal.

achieve a certain value of γ decreases with increasing ϵ and is in inverse proportion to θ_0. Note that θ_0 shows a nontrivial increase in the strongly nonlinear regime (Fig. 5). α is equal to $G\hat{T}_0/\Delta T$, where $\hat{T}_0$ is the amplitude of uncontrolled temperature oscillation computed from its rms value. This means that the necessary initial heater output ($G\hat{T}_0$) divided by the imposed temperature difference to achieve certain value of γ is independent of ϵ in this regime. Furthermore, the universal value of the optimal α is identified as $\alpha=0.04$. Hence, knowing the nondimensionalized amplitude of the uncontrolled temperature signal, the optimal value of G can be estimated. This allows the control scheme to be fully automatic in case of high ϵ.

The curves in the weakly nonlinear regime show different characteristics compared to the ones in the strongly nonlinear regime. In contrast to the strongly nonlinear regime, where the suppression rate γ suddenly drops to the minimum value with increasing α, γ drops rather slowly in the weakly nonlinear regime. This results in values of optimal α that are higher than the ones in the strongly nonlinear regime.

Figure 12 shows the performance of the control scheme for various ϵ. $\gamma(G_{optimal})$ is the value of γ when $G=G_{optimal}$. Observing the data from Sensor1 (circles), the control scheme shows excellent performance for the smallest $\epsilon=0.05$. Increasing ϵ, $\gamma(G_{optimal})$ increases proportional to ϵ. The trend changes when ϵ reaches around 0.35 that, as shown in Fig. 5, corresponds to the value of ϵ where $\hat{\theta}_0$ starts to fall below the bifurcation curve due to the strong nonlinearity. In the strongly nonlinear regime, the amplitude ratio is almost constant and below 35%.

Data from sensor 2 (stars) give some hints to grasp how the control influences the whole flow field. Note that sensor 2 was located 60° away from sensor 1 in the azimuthal direction, with the same radial position. Even though it is not as much as at the sensor 1 location, the control achieves suppression of the oscillation in sensor 2 location for the range of ϵ. Especially for the smallest $\epsilon=0.05$, considerable suppression of the oscillation [$\gamma(G_{optimal})=0.25$] was obtained. In the regime with weak nonlinearity, the trend of $\gamma(G_{optimal})$ correlates with those of Sensor1 to increase linearly with ϵ. $\gamma(G_{optimal})$ increases until it reaches its peak at ϵ 0.2$\sim$0.3, where the least suppression is obtained. As the nonlinearity becomes stronger, $\gamma(G_{optimal})$ decreases, which implies that the influence of the control becomes more global.

IV. CONCLUSIONS

Active control was applied to oscillatory thermocapillary flow in an annular configuration. Significant attenuation of the oscillation was achieved in a range of supercritical Marangoni numbers, with the best performance in the weakly nonlinear regime. There, the suppression ratio of the local oscillation amplitudes γ, increase as ϵ increases, while in the strongly nonlinear regime, γ is almost constant. The reliable temperature measuring technique enabled us to analyze the effect of the control method quantitatively. In the strongly nonlinear regime, a scaling of the feedback amplification was identified from which we could calculate the optimal gain. Measuring the temperature oscillation at two positions simultaneously gives us good insight in how the control influences the whole temperature field on the free surface.

In the work by Petrov *et al.* [19] of nonlinear control in a different geometry, the local oscillation could be almost completely suppressed for a fixed $\epsilon=0.27$. The advantage of the present method lies in its robustness where the control could be carried out in a wide range of $\epsilon(0.05\leqslant\epsilon\leqslant0.89)$ even though Petrov *et al.* have achieved lower controlled amplitude. Also the simplicity of the method allowed us to tackle the object without constructing the reference data before hand. $\epsilon=0.35$, where the characteristic of the controlled signal changed, corresponds to $\epsilon=0.36$(Ma=19 000) reported by Petrov *et al.* to be the limit above which the nonlinear control scheme fails because of strong nonlinearity of dynamics.

ACKNOWLEDGMENT

This work was supported by the Swedish Research Council for Engineering Sciences (TFR).

[1] M.K. Smith and S.H. Davis, J. Fluid Mech. **132**, 119 (1983a).
[2] R.J. Riley and G.P. Neitzel, J. Fluid Mech. **359**, 143 (1998).
[3] D. Schwabe and A. Scharmann, J. Cryst. Growth **46**, 125 (1979).
[4] S. Ostrach, Y. Kamotani, and C. Lai, PCH, PhysicoChem. Hydrodyn. **6**, 585 (1985).
[5] R. Velten, D. Schwabe, and A. Scharmann, Phys. Fluids A **3**, 267 (1991).
[6] C.-H. Chun and W. Wuest, Acta Astron. **6**, 1073 (1979).
[7] F. Preisser, D. Schwabe, and A. Scharmann, J. Fluid Mech.

126, 545 (1983).
[8] Y. Kamotani, J. Lee, S. Ostrach, and A. Pline, Phys. Fluids A **4**, 955 (1992).
[9] Y. Kamotani, J. Masud, and A. Pline, J. Thermophys. Heat Transfer **10**, 102 (1996b).
[10] Y. Kamotani, S. Ostrach, and J. Masud, J. Fluid Mech. **410**, 211 (2000).
[11] G.P. Neitzel, K.-T. Chang, D.F. Jankowski, and H.D. Mittelmann, Phys. Fluids A **5**, 108 (1993).
[12] H.C. Kuhlmann and H.J. Rath, J. Fluid Mech. **247**, 247 (1993).
[13] N.D. Kazarinoff and J.S. Wilkowski, Phys. Fluids A **1**, 625 (1989).
[14] N.D. Kazarinoff and J.S. Wilkowski, Phys. Fluids A **2**, 1797 (1990).
[15] R. Rupp, G. Muller, and G. Neumann, J. Cryst. Growth **97**, 34 (1989).
[16] M. Levenstam and G. Amberg, J. Fluid Mech. **297**, 357 (1995).
[17] M. Wanschura, V.M. Shvetsova, H.C. Kuhlmann, and H.J. Rath, Phys. Fluids **7**, 912 (1995).
[18] S. Benz, P. Hinz, R.J. Riley, and G.P. Neitzel, J. Fluid Mech. **359**, 165 (1998b).
[19] V. Petrov, M.F. Schatz, K.A. Muehlner, S.J. VanHook, W.D. McCormick, J.B. Swift, and H.L. Swinney, Phys. Rev. Lett. **77**, 3779 (1996).
[20] G. Iooss and D.D. Joseph, *Elementary Stability and Bifurcation Theory* (Springer-Verlag, Berlin, 1989).
[21] R. Lavalley, Technical Report No. TRITA-MEK 1997:20, Department of Mechanics, KH, 1997 (unpublished).
[22] R. Lavalley, G. Amberg, and P.H. Alfredsson, Eur. J. Mech. B/Fluids (to be published).